

# Theoretical Prediction of the Thermochemistry and Kinetics of Reactions of CF<sub>2</sub>O with Hydrogen Atom and Water

M. R. Zachariah,<sup>\*,†</sup> W. Tsang,<sup>†</sup> P. R. Westmoreland,<sup>‡</sup> and D. R. F. Burgess, Jr.<sup>†</sup>

National Institute of Standards and Technology, Gaithersburg, Maryland 20899-0001, and University of Massachusetts, Amherst, Massachusetts 01003-3110

Received: December 21, 1994; In Final Form: June 6, 1995<sup>⊗</sup>

A theoretical investigation of transition states and reaction products for reaction of carbonyl difluoride (CF<sub>2</sub>O) with H atoms and water has been conducted. Bond-additivity-corrected (BAC) MP4 calculations have been used to obtain the thermochemistry of equilibrium and transition state structures. RRKM/master equation as well as bimolecular-QRRK analysis of the H atom reaction manifold has been compared with available experimental rate constants and shows excellent agreement. The major reaction pathway is through attack on the oxygen, followed by chemically activated 1,2-elimination of HF. Analysis of carbonyl difluoride reaction with water indicates that the primary reaction is through a concerted reaction to form fluoroformic acid (FCO(OH)) and HF. Calculated rate constants for CF<sub>2</sub>O with water are considerably slower than reaction with H atoms, and even in hydrocarbon flames, where the water concentration is high, the H atom reaction should dominate. Reaction with OH was found not to be competitive with the other two processes and proceeds to FCO<sub>2</sub> + HF.

## Introduction

Carbonyl difluoride (CF<sub>2</sub>O) plays a key role in both atmospheric and plasma etching chemistry and flame suppression behavior of fluorocarbons. Accurate knowledge of the thermochemistry and kinetics is key to understanding its role in these disparate environments. Our interest in carbonyl difluoride is associated with its role in flames where halons have been added for flame suppression purposes<sup>1-5</sup> and its possible relevance to the chemistry of plasma etching using fluorocarbons.<sup>6</sup> At the high temperatures encountered in flames, CF<sub>2</sub>O is primarily formed through oxidation of the CF<sub>3</sub> radical by O, OH, and O<sub>2</sub>. Destruction of CF<sub>2</sub>O has been estimated to be primarily through reaction with H atoms,<sup>7,8</sup> but one might expect that, under certain circumstances, reaction with water (a major species in hydrocarbon flames) might be important as well. In this paper, we report calculations for the most likely reaction pathways for CF<sub>2</sub>O destruction from reaction with H and H<sub>2</sub>O through calculation of the thermochemistry, transition states, and master equation analysis for determination of kinetic rates.

## Computational Procedure

Calculations were performed using the bond-additivity-corrected MP4 (BAC-MP4) procedure outlined by Melius.<sup>9</sup> This procedure involves *ab initio* molecular orbital calculation using the Gaussian series of programs,<sup>10</sup> followed by a BAC procedure to the energy. The essence of the BAC procedure is to allow one to accurately calculate energies without the need to resort to large basis sets or configuration interaction terms. This is of particular importance when the goal is generation of a large body of data in the absence of a complete set of experimental thermochemical and kinetic data for a specific system.<sup>1</sup>

Equilibrium geometries, vibrational frequencies, and zero point energies were calculated at the HF/6-31G(d) level. Single-point energies were calculated at the MP4/6-31G(d,p) level, to

TABLE 1: Bond Additivity Correction Parameters

bond	calibration species	MP4/6-31G(d,p)//HF/6-31G(d)			
		A <sub>ij</sub>	α <sub>ij</sub>	atom type	B <sub>k</sub>
C-H	CH <sub>4</sub>	38.61	2.0	H	0
O-H	H <sub>2</sub> O	72.45	2.0	C	0.31
C-O	CH <sub>3</sub> OH, CH <sub>2</sub> O	175.6	2.14	O	0.225
H-F	HF	84.21	2.0	F	0.33
C-F	CF <sub>4</sub>	143.29	2.1		
H-H	H <sub>2</sub>	18.98	2.0		

which the BAC procedure was applied. In the BAC method, errors in the electronic energy of a molecule are treated as bondwise additive, depending only on the bonding partner and distance. The energy per bond is corrected by calibration at a given level of theory against molecules of known energy.

The transition state for a reaction was obtained in the usual way by searching for a geometry with one negative eigenvalue (saddle point on the potential energy surface), followed by steepest-descent reaction path analysis to ensure that the calculated transition state corresponds to the appropriate reactants and products. BAC corrections are assigned in the same manner as that with the equilibrium structure.

Melius and Binkley<sup>9</sup> have shown that for any molecule A<sub>k</sub>-A<sub>i</sub>-A<sub>j</sub>-A<sub>l</sub>, the error in calculating the electronic energy can be estimated through a pairwise additive bond correction E<sub>BAC</sub> of the form

$$E_{\text{BAC}}(A_i-A_j) = f_{ij}g_{kij}g_{ijl} \quad (1)$$

where

$$f_{ij} = A_{ij} \exp(-\alpha_{ij}r_{ij}) \quad (2)$$

A<sub>ij</sub> and α<sub>ij</sub> are calibration constants (shown in Table 1) that depend on bond type, r<sub>ij</sub> is the bond length at the Hartree-Fock level, and

$$g_{kij} = (1 - h_{ik}h_{ij}) \quad (3)$$

is the second nearest neighbor (to the bond being considered) correction where

\* To whom correspondence should be addressed.

† Mail stop 221/B312, National Institute of Standards and Technology.

‡ University of Massachusetts.

⊗ Abstract published in *Advance ACS Abstracts*, August 1, 1995.

$$h_{ik} = B_k \exp(-\alpha_{ik}(r_{ik} - (1.4 \text{ \AA}))) \quad (4)$$

For open-shelled molecules, an additional correction is needed due to contamination from higher spin states. This error is estimated using an approach developed by Schlegel<sup>11</sup> in which the spin energy correction is obtained from

$$E_{\text{spin}} = E(\text{UMP3}) - E(\text{PUMP3}) \quad (5)$$

For closed-shell species having a UHF instability

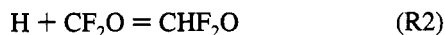
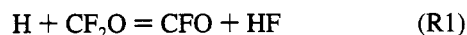
$$E_{\text{spin}} = KS(S + 1) \quad \text{where } K = 41.8 \text{ kJ/mol} \quad (6)$$

We have used this approach for the calculation of the thermochemistry for over 90 fluorocarbons, comparing the results where available with experimental data and finding an average deviation of approximately 6.7 kJ/mol.<sup>1,5</sup> Transition state structures were used directly to calculate the density of states necessary for RRKM and subsequent steady state master equation analysis, assuming a step-ladder model with a step-size down that follows the relation  $100(T/300) \text{ cm}^{-1}$ .<sup>12-15</sup>

## Results

**Thermochemistry of CF<sub>2</sub>O + H.** The high concentration of H atoms in flames where carbonyl difluoride is formed has led to a number of experimental determinations of the rate constants for the H + CF<sub>2</sub>O reaction.<sup>6,7</sup>

Reaction of H + CF<sub>2</sub>O could in principle involve direct abstraction, addition/stabilization or addition followed by chemically activated decomposition or isomerization through the following reactions:



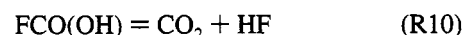
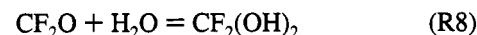
In order to make predictions of the rate constants for each of these channels, it is necessary to know the structure and energy of the transition states. Table 2 lists the relevant calculated energies, bond corrections, and thermochemistries for both equilibrium and transition state structures. Tables 3 and 4 list the calculate vibrational frequencies and moments of inertia, respectively. The potential energy curves for reactions R1–R6 are shown in Figure 1.

A key issue in this work has been the heat of formation of carbonyl difluoride. As previously mentioned, we have used the BAC procedure to calculate a large number of species thermochemistries that have subsequently been compared to literature values (average deviation 6.7 kJ/mol). The literature values include those calculated from heats of reaction or estimated using bond dissociation energies or group additivity.<sup>16</sup> Of the over 100 species calculated, carbonyl difluoride gave by far the largest apparent deviation of 37 kJ/mol in the heat of formation at standard state. The previously accepted JANAF value (based on the heat of hydrolysis of CF<sub>2</sub>O) is –635 kJ/mol, compared to our calculated value of –598 kJ/mol.

During the course of this work, we have used large basis sets and a limited number of G2 calculations to examine possible

errors due to insufficiently small basis sets, electron correlation, or the BAC corrections. However, two independent calculations cast doubt on the validity of the accepted JANAF number. Montgomery et al.<sup>17</sup> have recently completed a study of the thermochemistry of CF<sub>2</sub>O based on calculations using the CBS method and determined a value for the heat of formation at 298 K of –608.6 kJ/mol. More recently Schnieder and Wallington<sup>18</sup> conducted a study of the thermochemistry of CF<sub>2</sub>O and related compounds using QCI-based calculations and have concluded that the discrepancies they observe can only be explained from experimental error. They have recommended a value of  $-607.3 \pm 7$  kJ/mol in excellent agreement with the Montgomery et al.<sup>17</sup> work and consistent with our –598.2 kJ/mol value. On the basis of these three independent calculations, we proceed on the assumption that while one cannot conclude that the experimental number is wrong, it is unlikely that *ab initio* calculations using different approaches that have demonstrated high accuracy for other fluorocarbons should produce an error of the magnitude necessary for the JANAF assignment to be correct.

**Thermochemistry of CF<sub>2</sub>O + H<sub>2</sub>O.** High concentrations of water vapor produced during combustion make water a candidate for reaction with carbonyl difluoride. We have calculated thermochemistries for the following species and transition states shown in Figure 2.



The relevant energies and thermochemical properties are listed in Table 2.

Francisco<sup>19</sup> has recently made predictions for the thermochemistry of reactions R8–R10 at the MP2/6-311G\*\* level but did not address the possibility of reaction R7. In general, our calculations indicate lower barrier heights than those calculated in the Francisco study, presumably due to the higher levels of electron correlation used in this work. In particular, CF<sub>2</sub>(OH)<sub>2</sub> is considerably more stable relative to the other species in our calculations than that resulting from the Francisco study. In a more recent study Dibble and Francisco<sup>19</sup> report a value for the heat of formation (based on G2) for FCO(OH) of –614.0 kJ/mol, in excellent agreement with our number of –614.8 kJ/mol.

**Analysis of Rate Constants.** Rate constants for the multiple-channel reactions have been predicted from master equation analysis of both the CF<sub>2</sub>O + H and CF<sub>2</sub>O + H<sub>2</sub>O systems and summarized in Figures 3 and 4.

The potential energy diagram for hydrogen atom attack on carbonyl difluoride shown in Figure 1 indicates that there are three pathways for attack. The following is a summary of the approaches used in deriving the kinetics.

(a) The rate constant for direct F abstraction can be directly calculated by transition state theory<sup>12</sup> from the transition state properties derived from the BAC-MP4 results. The very high reaction barrier (150 kJ/mol) makes this a minor channel.

(b) Rate constants for the addition/elimination sequences have been calculated using an RRKM/master equation procedure. The specific processes covered are as follows.

(1) Addition of H to the oxygen forms chemically activated CF<sub>2</sub>OH\*. This addition may be followed by stabilization, reversion to reactants, or 1,2-HF elimination giving HF + CFO.

**TABLE 2: Energies, Bond Corrections, and Heats of Formation<sup>a</sup>**

	$E_{MP4}$	$E_{HF}$	$E_{ZP}$	$E_{BAC}$	$\Delta H^{o,298}$
species					
HF	-100.201 317	-100.011 551	0.009 926	57.0	-273.3
CF <sub>2</sub> O	-312.273 987	-311.615 295	0.015 788	99.4	-598.4
FCO	-212.585 648	-212.112 061	0.009 258	90.0	-182.8
CFO <sub>2</sub>	-287.630 585	-286.998 169	0.015 303	114.0	-336.9
CHF <sub>2</sub> O	-312.786 407	-312.147 064	0.027 076	111.5	-405.6
CF <sub>2</sub> OH	-312.797 791	-312.143 646	0.026 418	138.5	-463.1
F <sub>2</sub> C(OH) <sub>2</sub>	-388.527 222	-387.663 544	0.044 988	205.5	-903.0
FCO(OH) trans	-288.313 629	-287.639 526	0.029 603	156.2	-614.8
CF <sub>2</sub> O(OH)	-387.843 719	-387.025 391	0.031 379	161.8	-621.4
transition states					
CF <sub>2</sub> O + H = FCO + HF	-312.695 129	-312.010 590	0.014 983	146.1	-229.7
CF <sub>2</sub> O + H = CHF <sub>2</sub> O	-312.744 507	-312.083 466	0.017 969	121.0	-329.0
CF <sub>2</sub> O + H = CF <sub>2</sub> OH	-312.732 422	-312.068 115	0.017 076	137.5	-315.2
CHF <sub>2</sub> O = FCO + HF <sup>b</sup>	-312.724 996		0.020 44		-248.6
CF <sub>2</sub> OH = FCO + HF	-312.727 875	-312.046 967	0.019 965	141.5	-300.1
CHF <sub>2</sub> O = CF <sub>2</sub> OH	-312.731 049	-312.060 669	0.020 645	136.2	-301.9
CF <sub>2</sub> O + H <sub>2</sub> O = FCO(OH) + HF	-388.451 141	-387.553 467	0.040 118	207.3	-719.0
CF <sub>2</sub> O + H <sub>2</sub> O = F <sub>2</sub> C(OH) <sub>2</sub>	-388.450 500	-387.564 636	0.039 578	202.7	-714.4
F <sub>2</sub> C(OH) <sub>2</sub> = FCO(OH) + HF	-388.461 273	-387.578 461	0.039 367	209.8	-749.8
FCO(OH) = CO <sub>2</sub> + HF	-288.257 477	-287.555 054	0.022 956	160.5	-489.0
CF <sub>2</sub> O + OH = CF <sub>2</sub> O(OH)	-387.807 401	-386.968 231	0.027 455	173.4	-547.5
CF <sub>2</sub> O(OH) = CFO <sub>2</sub> + HF	-387.778 870	-386.936 951	0.025 320	168.0	-473.5

<sup>a</sup>  $E_{MP4}$  = MP4 energy (hartrees);  $E_{HF}$  = HF energy (hartrees);  $E_{ZP}$  = zero point energy (hartrees);  $E_{BAC}$  = bond additivity correction (kJ/mol);  $\Delta H^{o,298}$  = enthalpy of formation at 298 K (kJ/mol). <sup>b</sup> Transition state geometry at mp2/6-31g(D); no Hartree-Fock TS found;  $\Delta H^{o,298}$  for R4 based on  $E_{MP4}(\text{CHF}_2\text{O}) - E_{MP4}(\text{CHF}_2\text{O}=\text{FCO}+\text{HF})$ , calculated at MP4/6-31g(d,p)/MP2/6-31g(d).  $E_{MP4}(\text{CHF}_2\text{O})$  at MP4/6-31g(d,p)/MP2/6-31g(d) = -312.78892.

**TABLE 3: Vibrational Frequencies (cm<sup>-1</sup>)**

species	frequency
HF	3890
CF <sub>2</sub> O	563, 610, 779, 977, 1305, 1953
FCO	632, 1081, 1915
CFO <sub>2</sub>	486, 585, 761, 961, 1303, 1901
CHF <sub>2</sub> O	443, 499, 645, 1015, 1147, 1155, 1355, 1391, 2961
CF <sub>2</sub> OH	239, 480, 492, 674, 1042, 1105, 1284, 1370, 3667
F <sub>2</sub> C(OH) <sub>2</sub>	162, 338, 432, 449, 583, 595, 606, 880, 1101, 1153, 1158, 1408, 1451, 3658, 3658
FCO(OH) trans	545, 557, 607, 791, 965, 1215, 1398, 1882, 3642
CF <sub>2</sub> O(OH)	242, 348, 428, 561, 573, 606, 877, 1105, 1235, 1287, 1388, 3648
transition state	frequency
CF <sub>2</sub> O + H = FCO + HF	-2092, 230, 237, 508, 520, 573, 740, 1117, 1946
CF <sub>2</sub> O + H = CHF <sub>2</sub> O	-1464, 525, 528, 658, 705, 765, 967, 1273, 1622
CF <sub>2</sub> O + H = CF <sub>2</sub> OH	-1978, 322, 488, 538, 590, 881, 940, 1304, 1630
CHF <sub>2</sub> O = FCO + HF <sup>b</sup>	-645, 338, 494, 632, 840, 1018, 1087, 1635, 1966
CF <sub>2</sub> OH = FCO + HF	-1889, 262, 578, 637, 716, 924, 1192, 1563, 1951
CHF <sub>2</sub> O = CF <sub>2</sub> OH	-2341, 497, 505, 670, 675, 992, 1249, 1323, 2179
CF <sub>2</sub> O + H <sub>2</sub> O = FCO(OH) + HF	-1243, 311, 415, 439, 495, 536, 643, 740, 934, 1041, 1158, 1418, 1862, 2132, 3597
CF <sub>2</sub> O + H <sub>2</sub> O = F <sub>2</sub> C(OH) <sub>2</sub>	-1871, 336, 416, 435, 531, 571, 739, 801, 919, 1006, 1252, 1318, 1520, 2066, 3602
F <sub>2</sub> C(OH) <sub>2</sub> = FCO(OH) + HF	-1611, 234, 327, 463, 545, 547, 634, 863, 921, 988, 1188, 1430, 1625, 2040, 3623
FCO(OH) = CO <sub>2</sub> + HF	-1686, 374, 634, 651, 809, 1033, 1258, 2005, 2232
CF <sub>2</sub> O + OH = CF <sub>2</sub> O(OH)	-1259, 260, 309, 345, 503, 557, 582, 908, 955, 1299, 1462, 3579
CF <sub>2</sub> O(OH) = CFO <sub>2</sub> + HF	-1736, 254, 334, 464, 524, 655, 820, 943, 982, 1399, 1547, 2001

<sup>a</sup> Frequencies calculated at HF/6-31G(d) geometry and scaled by 0.89. <sup>b</sup> Frequencies calculated at MP2/6-31g(d).

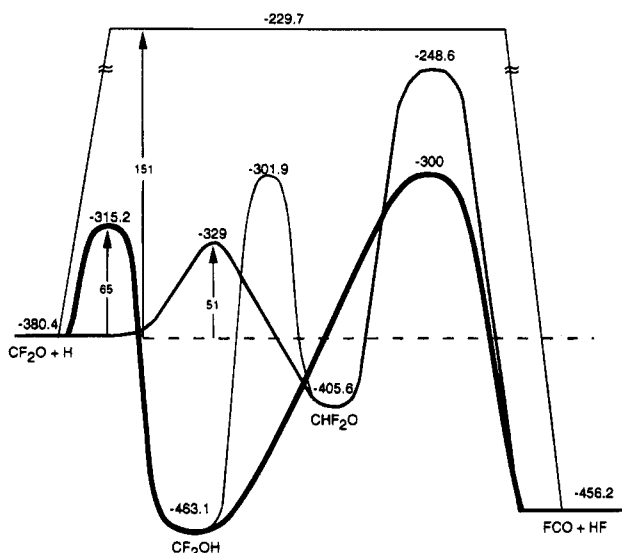
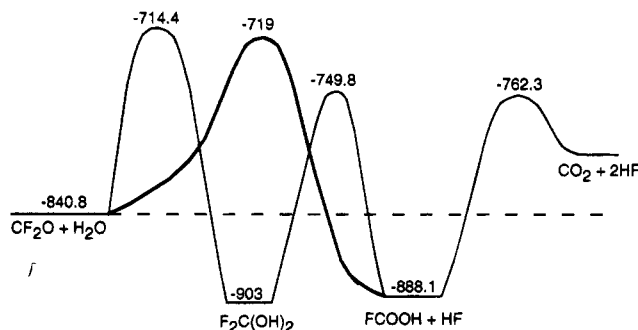
There is also an isomerization pathway leading to CHF<sub>2</sub>O\*, which can potentially decompose to the same products. However, the barrier going from CHF<sub>2</sub>O to HF and CFO products is 209 kJ higher than the reverse isomerization process. Furthermore, CF<sub>2</sub>OH is thermodynamically more stable than CHF<sub>2</sub>O, by a factor of 30 at 2000 K. Thus, conversion of the latter to the former is readily reversed. The consequence is that the presence of this isomerization channel can be ignored, and the calculated rate constant for H + CF<sub>2</sub>O is a minimum value. Opening up a new decomposition channel can only make the reverse decomposition (CF<sub>2</sub>OH = CF<sub>2</sub>O + H) less important. When this is coupled with the lower A-factor for isomerization as opposed to elimination and decomposition, it is clear that neglecting the former will introduce errors of only a few percent.

Preliminary time dependent reversible master equation analyses have corroborated this point.

Rate constants for the stabilization and chemically activated decomposition channels have been calculated on the basis of transition states for the formation of the adduct and its decomposition to HF + FCO and analyzed using an RRKM analysis and the steady state solution to the master equation with a step-ladder model. The step-size down for the model follows the relation  $100(T/300) \text{ cm}^{-1}$  and is based on correlations from hydrocarbon decomposition which are subject to uncertainties. However, as will be seen below, the rate constants are not sensitive to this parameter in the region of interest. In any case, setting the step-size down permits the description of the kinetic behavior of the entire system at any temperature or

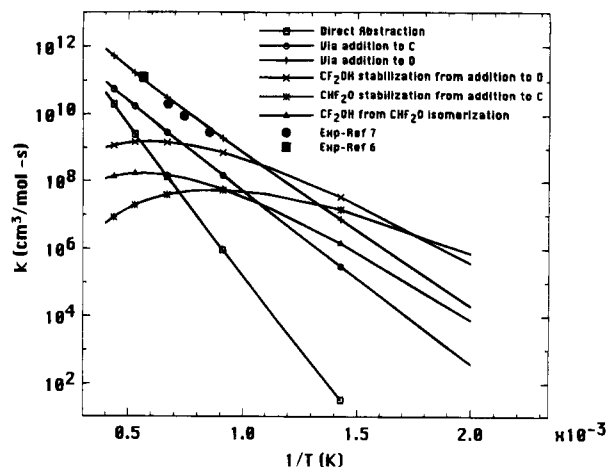
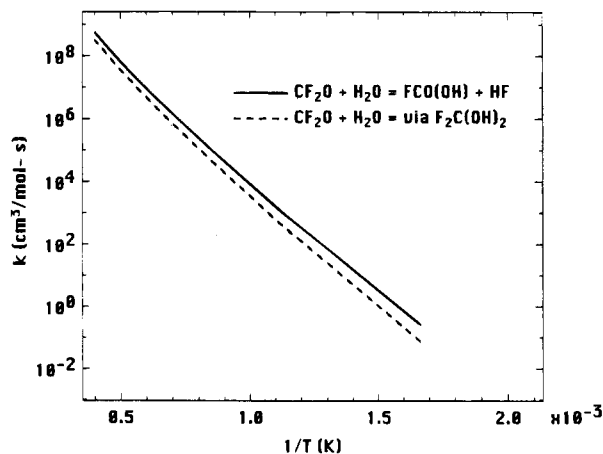
**TABLE 4: Moments of Inertia (cm<sup>2</sup> (10<sup>-40</sup>))**

species			
HF	0.0	1.3	1.3
CF <sub>2</sub> O	69.0	69.0	138.0
FCO	4.2	71.0	75.2
CFO <sub>2</sub>	63.4	69.9	133.3
CHF <sub>2</sub> O	76.2	78.5	141.7
CF <sub>2</sub> OH	74.7	78.3	147.9
F <sub>2</sub> C(OH) <sub>2</sub>	144.5	145.0	148.3
FCO(OH) trans	67.7	71.3	139.0
CF <sub>2</sub> O(OH)	138.1	139.2	147.2
transition states			
CF <sub>2</sub> O + H = FCO + HF	70.1	113.0	183.1
CF <sub>2</sub> O + H = CHF <sub>2</sub> O	75.6	75.8	140.9
CF <sub>2</sub> O + H = CF <sub>2</sub> OH	74.7	78.5	146.7
CHF <sub>2</sub> O = FCO + HF	76.5	96.1	166.9
CF <sub>2</sub> OH = FCO + HF	65.0	100.4	157.7
CHF <sub>2</sub> O = CF <sub>2</sub> OH	75.7	77.8	146.5
CF <sub>2</sub> O + H <sub>2</sub> O = FCO(OH) + HF	138.3	161.3	172.4
CF <sub>2</sub> O + H <sub>2</sub> O = F <sub>2</sub> C(OH) <sub>2</sub>	133.4	151.1	161.6
F <sub>2</sub> C(OH) <sub>2</sub> = FCO(OH) + HF	130.7	169.7	177.4
FCO(OH) = CO <sub>2</sub> + HF	60.3	95.4	155.8
CF <sub>2</sub> O + OH = CF <sub>2</sub> O(OH)	132.8	154.4	164.2
CF <sub>2</sub> O(OH) = CFO <sub>2</sub> + HF	125.7	160.8	172.0

**Figure 1.** Potential energy diagram for CF<sub>2</sub>O + H (kJ/mol).**Figure 2.** Potential energy diagram for CF<sub>2</sub>O + H<sub>2</sub>O (kJ/mol).

pressure. At the high temperatures of interest here, this leads to results for the chemically activated decomposition that are near the limiting low pressure value; i.e. they are independent of pressure and energy transfer effects. In contrast, the bimolecular rate constant is much lower and is in the falloff to the low pressure limit (proportional to pressure). The decomposition channel is the main chain channel of the two.

(2) Addition to the carbon forms chemically activated CHF<sub>2</sub>O\*: As noted earlier, its isomerization is strongly favored over direct decomposition of CHF<sub>2</sub>O to HF and FCO. We have

**Figure 3.** Predicted rate constants for the CF<sub>2</sub>O + H reaction manifold: comparison with experiment.**Figure 4.** Predicted rate constants for the CF<sub>2</sub>O + H<sub>2</sub>O reaction manifold.**TABLE 5: Calculated Reaction Rate Coefficients<sup>a</sup> (cm<sup>3</sup> s mol<sup>-1</sup>)**

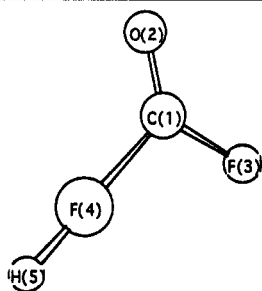
	A	n	E <sub>a</sub> /R
H + CF <sub>2</sub> O → FCO + HF (direct abstraction)	2.4 × 10 <sup>7</sup>	1.88	18060
H + CF <sub>2</sub> O → FCO + HF (addition to C)	1.2 × 10 <sup>10</sup>	0.83	11215
H + CF <sub>2</sub> O → FCO + HF (addition to O)	5.5 × 10 <sup>8</sup>	1.42	9532
H + CF <sub>2</sub> O → CF <sub>2</sub> OH (stabilization)	1.4 × 10 <sup>35</sup>	-7.08	12043
H + CF <sub>2</sub> O → CHF <sub>2</sub> O (stabilization)	6.3 × 10 <sup>40</sup>	-7.66	10795
H <sub>2</sub> O + CF <sub>2</sub> O → FCO(OH) + HF	7.4 × 10 <sup>-3</sup>	3.84	12611
H <sub>2</sub> O + CF <sub>2</sub> O → F <sub>2</sub> C(OH) <sub>2</sub>	3.0 × 10 <sup>-3</sup>	3.91	13079
OH + CF <sub>2</sub> O → CFO <sub>2</sub> + HF	2.7 × 10 <sup>3</sup>	2.38	10115

<sup>a</sup> Rate constants for 1 atm.

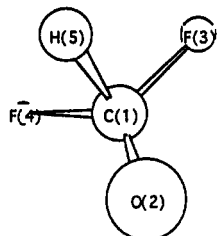
verified the unimportance of the direct CHF<sub>2</sub>O → HF + FCO channel in comparison to the isomerization below. A detailed master equation calculation involving hot molecules undergoing addition → reversible isomerization → decomposition is complex and beyond our present capabilities. We have used (i) unimolecular RRKM/master equation calculation to examine the influence of energy transfer on the rate constants and (ii) bimolecular quantum-RRK (QRRK)<sup>20</sup> to estimate the rate constants for the full sequence of chemically activated steps.

Our results are based on transition state calculations on the rate constants for CHF<sub>2</sub>O formation and its isomerization. From Figure 1 it can be seen that all the transition states are near the same level of excitation. We have therefore taken the ratio of decomposition to products to decomposition to reactants from the calculation in CF<sub>2</sub>OH decomposition and multiplied it by the isomerization rate constant to determine the ultimate rate

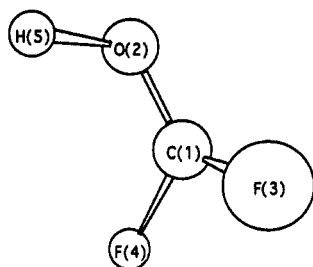
TABLE 6: Transition State Geometries

R1  $\text{H} + \text{CF}_2\text{O} = \text{CFO} + \text{HF}$ 

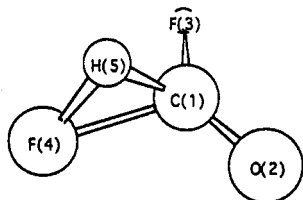
C(1)-O(2)=1.149; C(1)-F(3)=1.290; C(1)-F(4)=1.694; F(4)-H(5)=1.267  
 O(2)-C(1)-F(3)=128.79; O(2)-C(1)-F(4)=125.10; F(3)-C(1)-F(4)=106.11  
 C(1)-F(4)-H(5)=180.0; O(2)-C(1)-F(4)-H(5)=180.0; F(3)-C(1)-F(4)-H(5)=0.0

R2  $\text{H} + \text{CF}_2\text{O} = \text{CHF}_2\text{O}$ 

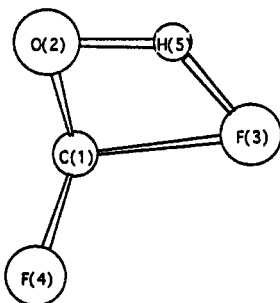
C(1)-O(2)=1.198; C(1)-F(3)=1.303; C(1)-F(4)=1.303; C(1)-H(5)=1.590  
 O(2)-C(1)-F(3)=123.32; O(2)-C(1)-F(4)=123.32; O(2)-C(1)-H(5)=93.03  
 F(3)-C(1)-F(4)=108.55; F(3)-C(1)-H(5)=99.70; F(4)-C(1)-H(5)=99.70

R3  $\text{H} + \text{CF}_2\text{O} = \text{CF}_2\text{OH}$  (mp2 geometry)

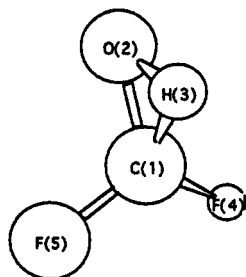
C(1)-O(2)=1.212; C(1)-F(3)=1.300; C(1)-F(4)=1.300; O(2)-H(5)=1.393  
 O(2)-C(1)-F(3)=122.67; O(2)-C(1)-F(4)=122.68; F(3)-C(1)-F(4)=110.04  
 C(1)-O(2)-H(5)=115.48; F(3)-C(1)-O(2)-H(5)=-76.77; F(4)-C(1)-O(2)-H(5)=76.75

R4  $\text{CHF}_2\text{O} = \text{CFO} + \text{HF}$ 

C(1)-O(2)=1.183; C(1)-F(3)=1.328; C(1)-F(4)=1.652; C(1)-H(5)=1.272; F(4)-H(5)=1.349  
 O(2)-C(1)-F(3)=128.32; O(2)-C(1)-F(4)=120.66; O(2)-C(1)-H(5)=121.13  
 F(3)-C(1)-F(4)=101.24; F(3)-C(1)-H(5)=107.59; F(4)-C(1)-H(5)=53.02  
 C(1)-F(4)-H(5)=48.91; C(1)-H(5)-F(4)=78.06; O(2)-C(1)-F(4)-H(5)=107.82  
 F(3)-C(1)-F(4)-H(5)=-103.65; O(2)-C(1)-H(5)-F(4)=-106.92; F(3)-C(1)-H(5)-F(4)=91.00

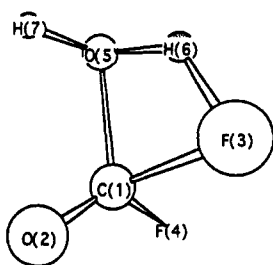
R5  $\text{CF}_2\text{OH} = \text{CFO} + \text{HF}$ 

C(1)-O(2)=1.238; C(1)-F(3)=1.709; C(1)-F(4)=1.279; O(2)-H(5)=1.215; F(3)-H(5)=1.180  
 O(2)-C(1)-F(3)=90.32; O(2)-C(1)-F(4)=123.82; F(3)-C(1)-F(4)=107.48  
 C(1)-O(2)-H(5)=81.29; C(1)-F(3)-H(5)=64.12; O(2)-H(5)-F(3)=124.15  
 F(3)-C(1)-O(2)-H(5)=2.19; F(4)-C(1)-O(2)-H(5)=113.62; O(2)-C(1)-F(3)-H(5)=-2.47  
 F(4)-C(1)-F(3)-H(5)=-128.30; C(1)-O(2)-H(5)-F(3)=-3.83; C(1)-F(3)-H(5)-O(2)=3.05

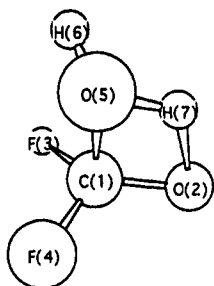
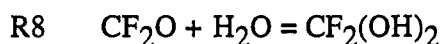
R6  $\text{CHF}_2\text{O} = \text{CF}_2\text{OH}$ 

C(1)-O(2)=1.313; C(1)-H(3)=1.288; C(1)-F(4)=1.309; C(1)-F(5)=1.309  
 O(2)-H(3)=1.204; O(2)-C(1)-H(3)=55.11; O(2)-C(1)-F(4)=117.20  
 O(2)-C(1)-F(5)=117.20; H(3)-C(1)-F(4)=123.32; H(3)-C(1)-F(5)=123.32  
 F(4)-C(1)-F(5)=109.61; C(1)-O(2)-H(3)=61.40; C(1)-H(3)-O(2)=63.48  
 F(4)-C(1)-O(2)-H(3)=-113.24; F(5)-C(1)-O(2)-H(3)=113.24  
 F(4)-C(1)-H(3)-O(2)=102.03; F(5)-C(1)-H(3)-O(2)=-102.03

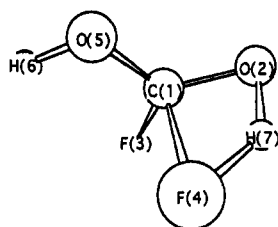
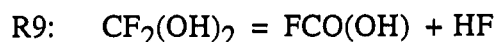
TABLE 6 (Continued)



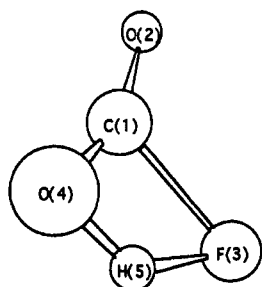
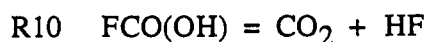
C(1)-O(2)=1.165; C(1)-F(3)=1.723; C(1)-F(4)=1.289; C(1)-O(5)=1.505  
 F(3)-H(6)=1.298; O(5)-H(6)=1.088; O(5)-H(7)=0.956; O(2)-C(1)-F(3)=115.33  
 O(2)-C(1)-F(4)=127.59; O(2)-C(1)-O(5)=118.64; F(3)-C(1)-F(4)=97.51  
 F(3)-C(1)-O(5)=81.63; F(4)-C(1)-O(5)=105.03; C(1)-F(3)-H(6)=69.68  
 C(1)-O(5)-H(6)=83.91; C(1)-O(5)-H(7)=107.48; H(6)-O(5)-H(7)=112.17  
 F(3)-H(6)-O(5)=124.73; O(2)-C(1)-F(3)-H(6)=-116.79; F(4)-C(1)-F(3)-H(6)=105.19  
 O(5)-C(1)-F(3)-H(6)=1.00; O(2)-C(1)-O(5)-H(6)=113.22; O(2)-C(1)-O(5)-H(7)=1.87  
 F(3)-C(1)-O(5)-H(6)=-1.14; F(3)-C(1)-O(5)-H(7)=-112.50; F(4)-C(1)-O(5)-H(6)=-96.71  
 F(4)-C(1)-O(5)-H(7)=151.92; C(1)-F(3)-H(6)-O(5)=-1.67; C(1)-O(5)-H(6)-F(3)=1.79  
 H(7)-O(5)-H(6)-F(3)=108.23



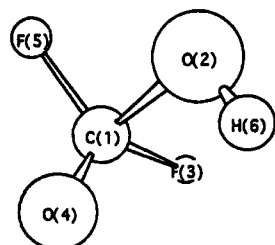
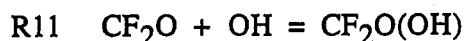
C(1)-O(2)=1.259; C(1)-F(3)=1.322; C(1)-F(4)=1.306; C(1)-O(5)=1.547  
 O(2)-H(7)=1.334; O(5)-H(6)=0.955; O(5)-H(7)=1.153; O(2)-C(1)-F(3)=119.27  
 O(2)-C(1)-F(4)=119.86; O(2)-C(1)-O(5)=96.16; F(3)-C(1)-F(4)=107.17  
 F(3)-C(1)-O(5)=15.36; F(4)-C(1)-O(5)=10.56; C(1)-O(2)-H(7)=77.04  
 C(1)-O(5)-H(6)=113.63; C(1)-O(5)-H(7)=71.88; H(6)-O(5)-H(7)=116.70  
 O(2)-H(7)-O(5)=114.76; F(3)-C(1)-O(2)-H(7)=109.09; F(4)-C(1)-O(2)-H(7)=-115.50  
 O(5)-C(1)-O(2)-H(7)=-2.36; O(2)-C(1)-O(5)-H(6)=114.71; O(2)-C(1)-O(5)-H(7)=2.81  
 F(3)-C(1)-O(5)-H(6)=-7.94; F(3)-C(1)-O(5)-H(7)=-119.83; F(4)-C(1)-O(5)-H(6)=-121.59  
 F(4)-C(1)-O(5)-H(7)=126.51; C(1)-O(2)-H(7)-O(5)=3.48; C(1)-O(5)-H(7)-O(2)=-2.90  
 H(6)-O(5)-H(7)-O(2)=-110.83



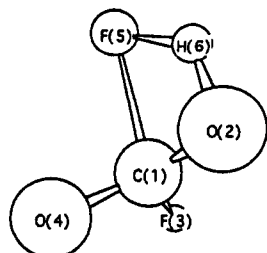
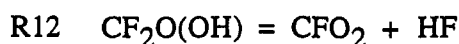
C(1)-O(2)=1.251; C(1)-F(3)=1.290; C(1)-F(4)=1.839; C(1)-O(5)=1.283  
 O(2)-H(7)=1.134; F(4)-H(7)=1.248; O(5)-H(6)=0.952; O(2)-C(1)-F(3)=120.27  
 O(2)-C(1)-F(4)=85.47; O(2)-C(1)-O(5)=121.92; F(3)-C(1)-F(4)=98.60  
 F(3)-C(1)-O(5)=113.84; F(4)-C(1)-O(5)=106.34; C(1)-O(2)-H(7)=86.28  
 C(1)-F(4)-H(7)=60.32; C(1)-O(5)-H(6)=111.88; O(2)-H(7)-F(4)=127.91  
 F(3)-C(1)-O(2)-H(7)=-96.72; F(4)-C(1)-O(2)-H(7)=0.54; O(5)-C(1)-O(2)-H(7)=107.05  
 O(2)-C(1)-F(4)-H(7)=-0.63; F(3)-C(1)-F(4)-H(7)=119.34; O(5)-C(1)-F(4)-H(7)=-122.60  
 O(2)-C(1)-O(5)-H(6)=180.0; F(3)-C(1)-O(5)-H(6)=21.860; F(4)-C(1)-O(5)-H(6)=-85.56  
 C(1)-O(2)-H(7)-F(4)=-1.09; C(1)-F(4)-H(7)-O(2)=0.89



C(1)-O(2)=1.131; C(1)-F(3)=1.754; C(1)-O(4)=1.226; F(3)-H(5)=1.244  
 O(4)-H(5)=1.136; O(2)-C(1)-F(3)=117.32; O(2)-C(1)-O(4)=155.32  
 F(3)-C(1)-O(4)=87.36; C(1)-F(3)-H(5)=62.84; C(1)-O(4)-H(5)=86.67  
 F(3)-H(5)-O(4)=123.11; O(2)-C(1)-F(3)-H(5)=-180.0; O(4)-C(1)-F(3)-H(5)=0.0  
 O(2)-C(1)-O(4)-H(5)=-180.0; F(3)-C(1)-O(4)-H(5)=0.0; C(1)-F(3)-H(5)-O(4)=0.0  
 C(1)-O(4)-H(5)-F(3)=-0.31



C(1)-O(2)=1.721; C(1)-F(3)=1.303; C(1)-O(4)=1.218; C(1)-F(5)=1.296  
 O(2)-H(6)=0.958; O(2)-C(1)-F(3)=103.59; O(2)-C(1)-O(4)=94.02  
 O(2)-C(1)-F(5)=101.18; F(3)-C(1)-O(4)=121.10; F(3)-C(1)-F(5)=108.85  
 O(4)-C(1)-F(5)=122.17; C(1)-O(2)-H(6)=107.07; F(3)-C(1)-O(2)-H(6)=-72.72  
 O(4)-C(1)-O(2)-H(6)=50.62; F(5)-C(1)-O(2)-H(6)=174.54



C(1)-O(2)=1.251; C(1)-F(3)=1.279; C(1)-O(4)=1.300; C(1)-F(5)=1.784; O(2)-H(6)=1.163  
 F(5)-H(6)=1.215; O(2)-C(1)-F(3)=123.08; O(2)-C(1)-O(4)=120.26; O(2)-C(1)-F(5)=86.66  
 F(3)-C(1)-O(4)=111.36; F(3)-C(1)-F(5)=100.12; O(4)-C(1)-F(5)=107.22  
 C(1)-O(2)-H(6)=84.86; C(1)-F(5)-H(6)=62.51; O(2)-H(6)-F(5)=125.92  
 F(3)-C(1)-O(2)-H(6)=98.87; O(4)-C(1)-O(2)-H(6)=-109.06; F(5)-C(1)-O(2)-H(6)=-1.04  
 O(2)-C(1)-F(5)-H(6)=1.09; F(3)-C(1)-F(5)-H(6)=-21.90; O(4)-C(1)-F(5)-H(6)=121.81  
 C(1)-O(2)-H(6)-F(5)=1.87; C(1)-F(5)-H(6)-O(2)=-1.48

constants to HF + CFO; i.e. the ultimate rate of CFO formation from CF<sub>2</sub>O + H (via hot CHF<sub>2</sub>O) is the rate of isomerization of CHF<sub>2</sub>O (since the direct decomposition to CFO is unfavored), multiplied by the fraction of the hot CF<sub>2</sub>OH that go to CFO as opposed to CF<sub>2</sub>O. Specifically,

$$k(\text{CHF}_2\text{O} \rightarrow \text{HF} + \text{CFO}) = [k(\text{CF}_2\text{OH} \rightarrow \text{HF} + \text{CFO}) / k(\text{CF}_2\text{OH} \rightarrow \text{H} + \text{CF}_2\text{O})] k(\text{CHF}_2\text{O} \rightarrow \text{CF}_2\text{OH})$$

$$k(\text{CF}_2\text{O} + \text{H} \rightarrow \text{HF} + \text{CFO}; \text{via CHF}_2\text{O}) = k(\text{CF}_2\text{O} + \text{H} \rightarrow \text{CF}_2\text{OH}^*) k(\text{CHF}_2\text{O} \rightarrow \text{HF} + \text{CFO})$$

Results can be found in Figure 3. The contributions from this channel are a factor of 30 to 10 smaller than those from b in the temperature range 600–2400 K. Note that, as in case b, reactions are at the low pressure limit under the combustion conditions of interest here and there are no energy transfer effects.

Our calculations also yield pressure dependent rate constants for CF<sub>2</sub>OH and CHF<sub>2</sub>O formation. The dominant channels are decompositions of chemically activated adduct back to the reactants because these are the lowest energy channels. In any case, under combustion conditions yields are sufficiently small that addition/stabilization does not contribute to the overall process. Thus in all the cases studied, the recommended rate constant is a measure of the partitioning of the initial addition product into a particular product channel where all possible decomposition channels, including the reverse process (in these cases H + CF<sub>2</sub>O), are considered.

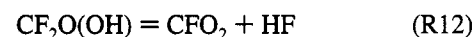
The complete set of rate constants was calculated using bimolecular quantum-RRK. This method has been shown to give good accuracy using a single, mean rovibrational frequency to introduce the necessary quantized energy effect into the chemically activated energy distribution and the  $k(E)$ 's. Key inputs were Arrhenius parameters evaluated at 1000 K from transition state theory and the BAC-MP4 calculations and a modified strong-collision model ( $k_{\text{stab}} = \beta Z[MM]$ ), which tend to overpredict stabilization.

Results were almost coincident with the estimates described above and in Figure 3. These QRRK results necessarily use less precise  $k(E)$ 's and no state-to-state energy transfer but do consider all accessible chemically activated pathways. The mutual agreement of the two analyses supports predicted rate constants and the analysis that at flame temperatures the primary pathway for reaction of CF<sub>2</sub>O + H reacts via addition to O, followed promptly by chemically activated 1,2-elimination of HF.

For this particular system, rate constants for the destruction of CF<sub>2</sub>O from H atoms have previously been estimated from experimental measurements of CF<sub>2</sub>O disappearance in flames. In their seminal study of molecular beam sampling in low pressure CF<sub>3</sub>Br-doped flames, Biordi et al.<sup>7</sup> measured both H atom and carbonyl difluoride and inferred a rate constant of  $1.3 \times 10^{11} \text{ cm}^3 \text{ mol}^{-1} \text{ s}^{-1}$  at 1800 K. Most recently the Vandoooren/Van Tiggelen group<sup>8</sup> have looked at CF<sub>3</sub>H combustion and estimated the rate as well. Their measured rate constants are shown in Figure 3 as well. Excellent agreement is clearly evident between both experimental data sources and between experiment and our calculations.

The results on carbonyl difluoride are in striking contrast to the situation for hydrogen atom attack on formaldehyde. The C–H bond in formaldehyde is extremely weak, the BDE being 364 kJ/mol as compared to the C–F BDE in carbonyl difluoride of 495 kJ/mol. The consequence is a rate expression<sup>21</sup> for hydrogen abstraction of  $2.2 \times 10^8 T^{1.77} \exp(-1510/T) \text{ cm}^3 \text{ mol}^{-1}$

$\text{s}^{-1}$ . Over all applicable temperature ranges, this expression leads to much larger rate constants for H + H<sub>2</sub>CO than our estimate for reaction of hydrogen with the perfluoro compound. Thus, commensurately less formaldehyde can be expected to survive under the conditions of interest here. Note that the weak C–H bond also leads to extremely rapid rate constants for OH attack on CH<sub>2</sub>O. The recommended rate expression<sup>21</sup> is  $3.4 \times 10^9 T^{1.18} \exp(2225/T) \text{ cm}^3 \text{ mol}^{-1} \text{ s}^{-1}$ . Thus, very little of the formaldehyde can have escaped from the oxidizing region. In contrast, we have computed the reaction of OH reaction with carbonyl difluoride in which the adduct CF<sub>2</sub>O(OH) ( $\Delta H^{\circ}_{f,298} = -621 \text{ kJ/mol}$ ) is formed and subsequently undergoes HF elimination to yield CFO<sub>2</sub> ( $\Delta H^{\circ}_{f,298} = -80 \text{ kJ/mol}$ ).



We obtain a calculated rate expression of  $2.3 \times 10^3 T^{2.38} \exp(-10115/T) \text{ cm}^3 \text{ mol}^{-1} \text{ s}^{-1}$ , which is more than a factor of 100 slower than the H atom case for temperatures below 2000 K. The species CFO<sub>2</sub> will be destroyed either via F atom elimination (C–F BDE = 320 kJ/mol) or through reaction with H atoms to yield CO<sub>2</sub> + HF.

For the reaction of CF<sub>2</sub>O with water, we used the potential energy diagram as outlined in Figure 2. As in the hydrogen case, there is a direct route as well as an indirect mechanism involving an intermediate complex. However, unlike the H atom attack case, the direct mechanism (CF<sub>2</sub>O + H<sub>2</sub>O → FCO(OH) + HF) leads to a rate constant that is larger than that for addition (CF<sub>2</sub>O + H<sub>2</sub>O → CF<sub>2</sub>(OH)<sub>2</sub>) as a result of the somewhat lower barrier and looser transition state. The results can be found in Figure 4. In trying to compare the analogous reactions with formaldehyde, we note that the hydrogen analogue of difluorodihydroxy methane is the stable form of formaldehyde seen in aqueous solution;<sup>22</sup> however, there does not appear to be any evidence for its presence in the gas phase.

In comparison to the data in Figure 3, it can be seen that the rate constants for reaction with water are factors of 2500–16 000 smaller in the temperature range of 1400–2200 K than those from reaction with H atoms. One should therefore expect that the water reaction will be a minor channel in the main reaction zone of a flame (despite concentrations 10–100 times greater than H atom) and would only compete with H atom attack at long residence times in the postflame where H atom concentration is low.

The rate constants computed in this work are tabulated in Table 5, and the transition state geometries are shown in Table 6.

## Conclusions

In this work, the reactions of carbonyl difluoride with hydrogen atom and water have been studied. A bond additivity correction procedure has been applied to *ab initio* molecular orbital calculations to obtain the thermochemistry for both equilibrium and transition state structures. These calculations have been used as the inputs to RRKM/master equation analysis and bimolecular quantum-RRK analysis to obtain the rate constants for the manifold of direct abstraction, addition/stabilization and addition/chemically activated decomposition reactions. Reaction with H atom proceeds primarily through addition to the oxygen, followed by chemically activated elimination of HF. The results compare extremely well with experimentally derived rate constants under flame conditions. Reaction with water is predicted to be considerably slower and

proceeds through a concerted reaction leading to FCO(OH) and HF, as does the reaction with OH leading to FCO<sub>2</sub> + HF.

**Acknowledgment.** We express our gratitude to Dr. Carl F. Melius of Sandia National Laboratories for the use of the BAC code and to Professor P. Van Tigglen for sharing ref 8 prior to publication.

### References and Notes

- (1) Nyden, M. D.; Linteris, G. T.; Burgess, D., Jr.; Westmoreland, P. R.; Tsang, W.; Zachariah, M. R. Flame Inhibition Chemistry and the Search for Additional Fire Fighting Chemicals. In *Evaluation of Alternative In-Flight Fire Suppressants for Full-Scale Testing in Simulated Aircraft Engine Nacelles and Dry Bays*; Grosshandler, W., Gann, R., Pitts, W., Eds.; Report # NIST SP 861; National Institute of Standards and Technology: 1994; pp 467-641.
- (2) Burgess, D., Jr.; Tsang, W.; Zachariah, M. R.; Westmoreland, P. R. *Prepr. Pap.-Am. Chem. Soc., Div. Fuel Chem.* **1994**, *39*, 141. Burgess, D. R. F., Jr.; Zachariah, M. R.; Tsang, W.; Westmoreland, P. R. Key Species and Important Reactions in Fluorinated Hydrocarbon Flame Chemistry. To be published in *ACS Symposium on Halon Replacements: Technology and Science*.
- (3) Westmoreland, P. R.; Burgess, D. R. F., Jr.; Tsang, W.; Zachariah, M. R., Kinetics of Fluoromethanes in Flames. *25th Symposium (International) on Combustion*; Combustion Institute: Pittsburgh, PA, 1994, p 1505.
- (4) Burgess, D. R. F., Jr.; Tsang, W.; Zachariah, M. R.; Westmoreland, P. R. *Proceedings of the Halon Options Technical Working Conference*; 1994; pp 489-501.
- (5) Zachariah, M. R.; Westmoreland, P. R.; Burgess, D. R. F., Jr.; Tsang, W.; Melius, C. F. Theoretical Prediction of Thermochemistry and Kinetics of Halocarbons. To be published in *ACS Symposium on Halon Replacements: Technology and Science*.
- (6) McMillin, B. K.; Zachariah, M. R. *J. Appl. Phys.* **1995**, *77*, 5538. McMillin, B. K.; Zachariah, M. R. 2-Dimensional, Argon Metastable Density Measurement in an RF Glow Discharge by Planar Laser Induced Fluores-

cence Imaging: Effect of CF<sub>4</sub>, O<sub>2</sub>, Cl<sub>2</sub>. Submitted for publication in *J. Appl. Phys.* McMillin, B. K.; Zachariah, M. R. 2-D Imaging of CF<sub>2</sub> by Laser-Induced Fluorescence of CF<sub>4</sub> Etching Plasmas in the GEC rf Reference Cell. *Proceedings of the 12th International Symposium on Plasma Chemistry*, Minneapolis, MN, Aug 21-25, 1995; 1995.

- (7) Biordi, J. C.; Lazzara, C. P.; Papp, J. F. *15th Symposium (International) on Combustion*; Combustion Institute: Pittsburgh, PA, 1974; p 917.
- (8) Richter, H.; Vandooren, J.; Van Tiggelen, P. J. *J. Chim. Phys., Phys.-Chim. Biol.* **1994**, *91*, 1748.
- (9) Melius, C. F.; Binkley, J. S. *21st Symposium (International) on Combustion*; Combustion Institute: Pittsburgh, PA, 1986; p 1953.
- (10) Frish, M. J.; Head-Gordon, M.; Trucks, G. W.; Foresman, J. B.; Schlegel, H. B.; Raghavachari, K.; Robb, M. A.; Binkley, J. S.; Gonzalez, C.; DeFrees, D. J.; Fox, D. J.; Whiteside, R. A.; Seeger, R.; Melius, C. F.; Baker, J.; Martin, L. R.; Kahn, L. R.; Stewart, J. J. P.; Topiol, S.; Pople, J. A. *Gaussian90*; Gaussian Inc.: Pittsburgh, PA, 1990.
- (11) Schlegel, H. B. *J. Chem. Phys.* **1986**, *84*, 4530.
- (12) Benson, S. W. *Thermochemical Kinetics*. Wiley, New York, 1974.
- (13) Robinson, P. J.; Holbrook, K. A. *Unimolecular Reactions*; Wiley Interscience: New York, 1972.
- (14) Tsang, W. *Combust. Flame* **1989**, *78*, 71.
- (15) Zachariah, M. R.; Tsang, W. *J. Phys. Chem.* **1995**, *99*, 5308.
- (16) Burgess, D. R. F., Jr.; Zachariah, M. R.; Tsang, W.; Westmoreland, P. R. Thermochemical and Kinetic Data for Fluorocarbons. *NIST Technical Note* 1412, 1995.
- (17) Montgomery, J. A., Jr.; Michels, H. H.; Francisco, J. S. *Chem. Phys. Lett.* **1994**, *220*, 391.
- (18) Schnieder, W. F.; Wallington, T. J. *J. Phys. Chem.* **1994**, *98*, 7448.
- (19) Francisco, J. S. *J. Atmos. Chem.* **1993**, *13*, 285. Dibble, T. S.; Francisco, J. S. *J. Phys. Chem.* **1994**, *98*, 11694.
- (20) Dean, A. M. *J. Phys. Chem.* **1992**, *89*, 151. Westmoreland, P. R. *Combust. Sci. Technol.* **1992**, *82*, 151.
- (21) Tsang, W.; Hampson, R. F. *J. Phys. Chem. Ref. Data* **1986**, *15*, 1087.
- (22) Noller, C. "The Chemistry of Organic Compounds", Saunders and Co., New York, 1951.

JP9433721